

CPT tests with the antihydrogen molecular ion

Edmund G. Myers

Department of Physics, Florida State University, Tallahassee, Florida 32306-4350, USA

(Received 2 January 2018)

High precision radio-frequency, microwave and infrared spectroscopic measurements of the antihydrogen molecular ion \bar{H}_2^- ($\bar{p}\bar{p}e^+$) compared with its normal matter counterpart provide direct tests of the CPT theorem. The sensitivity to a difference between the positron/antiproton and electron/proton mass ratios, and to a difference between the positron-antiproton and electron-proton hyperfine interactions, can exceed that obtained by comparing antihydrogen with hydrogen by several orders of magnitude. Practical schemes are outlined for measurements on a single \bar{H}_2^- ion in a cryogenic Penning trap, that use non-destructive state identification by measuring the cyclotron frequency and bound-positron spin-flip frequency; and also for creating an \bar{H}_2^- ion and initializing its quantum state.

Violation of the CPT theorem, which postulates invariance under the combined transformations of charge conjugation, parity and time-reversal would have profound consequences for all quantum field theories and fundamental physics [1–4]. A consequence of CPT is that the properties of fundamental particles and their antimatter conjugates should be identical except for the reversal of certain quantum numbers. This has led to much effort to compare precisely the masses and magnetic moments of the electron and positron [5–7], and of the proton and antiproton [8–12], and even greater efforts to compare the properties of hydrogen and antihydrogen [13–19].

In the case of antihydrogen (\bar{H}), the aim is to measure the $1s_{1/2}$ to $2s_{1/2}$ transition by two-photon (2E1) laser spectroscopy, and the $1s_{1/2}$ groundstate hyperfine splitting (HFS) by microwave spectroscopy, as well as to search for gravitational anomalies [20, 21]. For the $1s - 2s$ transition, the \bar{H} - H comparison is sensitive to the difference $q(e^+)^4m(e^+) - q(e^-)^4m(e^-)$, where $q(e^\pm)$, $m(e^\pm)$ are the respective charges and masses of the positron and electron. While there is also sensitivity to $m(e^+)/m(\bar{p}) - m(e^-)/m(p)$ through the reduced mass correction, this is decreased by a factor of $1/1836$. In the case of the HFS, the comparison is sensitive to a difference in the product of the positron(electron) and antiproton(proton) magnetic moments. \bar{H} has the attraction of the possibility of very high precision: for H , using cryogenically cooled beams, a fractional uncertainty of 4×10^{-15} has been achieved for the $1s - 2s$ transition [22], and 2.7×10^{-9} for the $1s$ HFS transition [23]. However, besides the difficulties of making \bar{H} , which currently proceeds by combining antiprotons from the Antiproton Decelerator (AD) at CERN [24] with positrons in nested Penning traps [25], experiments with \bar{H} suffer from the difficulty that it must be isolated from ordinary matter. Hence, spectroscopic experiments on \bar{H} use weak, large ($\gtrsim 100 \text{ cm}^3$) volume, neutral atom traps, such as the Ioffe-Pritchard trap [26–28], or tenuous beams [19], which pose difficulties for high precision. These include very low densities, inhomogeneous magnetic fields, Doppler shifts, and short transit times. So, although the first measure-

ments of the $1s - 2s$ [17] and $1s$ HFS [18] transitions in \bar{H} have already been made, and major improvements can be expected from laser cooling [29, 30], the precision achieved in hydrogen will not be reached for some years.

In contrast to the difficulties of confining antihydrogen, antiprotons (and normal matter ions) have long been trapped [31, 32] and are now routinely manipulated within [8, 33, 34] and between [11, 35, 36] cryogenic Penning traps for periods of many months, and they can be tightly confined, and their motions precisely monitored using image-current techniques [32, 37]. This encourages consideration of testing CPT by performing precise spectroscopy on the antihydrogen molecular ion \bar{H}_2^- , the simplest antiprotonic ion with discrete energy levels. Here it is shown, using non-destructive single ion detection techniques, that high-precision measurements on \bar{H}_2^- are possible. Specifically, methods are outlined for the measurement of bound-positron spin-flip (Zeeman) frequencies, Zeeman-hyperfine frequencies, and vibrational frequencies using Penning traps, that could enable tests of CPT using \bar{H}_2^- that are several orders-of-magnitude more sensitive than can be obtained with bare antiprotons or antihydrogen. This sensitivity advantage is particularly great for measurements of the hyperfine interaction, due to the long coherent interrogation times enabled by a Penning trap; and for measurements of vibrational transitions, which are inherently $\sim 10^3$ more sensitive to $m(e^+)/m(\bar{p}) - m(e^-)/m(p)$ than $1s - 2s$ spectroscopy in \bar{H} and H .

Energy levels: The H_2^+ (\bar{H}_2^-) ion in its ground electronic state $1s\sigma_g(X^2\Sigma_g^+)$ is strongly bound (dissociation energy $D_0 = 2.6507 \text{ eV}$), with 20 bound vibrational levels (quantum number v) and 423 bound rotational levels (quantum number N) [38–40]. The vibrational level spacing is 65.7 THz for $(v, N) = (0, 0)$ to $(1, 0)$. The number of bound rotational levels for each vibrational level decreases from 35 for $v = 0$, to 2 for $v = 19$. The rotational levels have para (ortho) exchange symmetry, with total nuclear spin $I = 0(1)$, for N even(odd). Because para-ortho transitions are strongly forbidden, the

N even and N odd ions are effectively separate species. For N even, the HFS is due only to the electron-spin molecular-rotation interaction. For odd N , the hyperfine structure is more complicated due to the additional interactions involving nuclear spin. However, in the 1 to 10 tesla magnetic fields of typical Penning traps, the Zeeman structure is in the strong-field regime, and the individual substates can be identified by the projections of the electron spin, total nuclear spin (if present), and rotational angular momentum, M_S , M_I , M_N . The Zeeman splitting with respect to M_S is dominant.

Since electric dipole transitions are forbidden in a homonuclear diatomic molecule, the ro-vibrational levels mainly decay by electric quadrupole (E2) transitions with selection rule $\Delta N = 0, \pm 2$. Excited vibrational levels have mean lifetimes on the order of a week or longer [41]. The rotational levels of $v = 0$ have mean lifetimes of a few days for N around 30, increasing to 3300 years for $N = 2$ [42] ($N = 0$ to 2 spacing 5.22 THz), while the radiative decay of $N = 1$ is forbidden. Hence $H_2^+(\bar{H}_2^-)$ has an abundance of transitions with extremely narrow radiative widths. This gives it an advantage for ultra-high precision spectroscopy relative to $H(\bar{H})$, whose only metastable levels are the upper hyperfine level of the ground state, and the $2s$ level, which has a lifetime of about 1/8 sec. On the other hand, compared to H , and to most atomic ions used for optical clocks, [43, 44], the lack of any electric dipole transition poses challenges by preventing direct laser cooling and state detection using fluorescence.

Single \bar{H}_2^- ion in a Penning trap: Here we focus on measurements that can be carried out in Penning traps that are compatible with current methods for trapping antiprotons [35]. In a precision Penning trap [32, 37], a set of cylindrically symmetric electrodes produces a quadrupolar electrostatic potential aligned with a highly uniform magnetic field. A single ion undergoes an axial motion parallel to the magnetic field due to the electrostatic potential, and two circular motions perpendicular to the magnetic field, the (modified) cyclotron motion and the magnetron motion. Using image-current techniques, the motions of a single ion can be cooled into thermal equilibrium with a high quality-factor inductor maintained at LHe temperature (4.2K) in time scales of 0.1 to 30 s. In the near future, by directly cooling the inductor with a dilution refrigerator, *e.g.*, see [45], or by using laser-cooled alkaline-earth ions in an adjacent trap with shared electrodes [46, 47], or laser-cooled anions in the same trap [48, 49], the \bar{H}_2^- ion temperature may be reduced by a further two to three orders of magnitude. Because of the difficulty of making \bar{H}_2^- ions, state detection and preparation methods are devised that enable measurements on a single \bar{H}_2^- to be repeated indefinitely. In particular, they do not use annihilation or photo-dissociation. In what follows, \bar{H}_2^- is referred to with the understanding that the same measurements can

(and more easily) be made on H_2^+ .

Bound positron g -factor: The first of the proposed measurements on \bar{H}_2^- , which also introduces the main state detection technique, is the simultaneous measurement of the bound-positron spin-flip frequency and ion cyclotron frequency, whose ratio is proportional to the positron g -factor. Although the measurement can be performed on an \bar{H}_2^- in essentially any (v, N) , it is simplest to consider the case of $N = 0$, where there is no hyperfine structure. The Zeeman structure then consists of two states with $M_S = \pm 1/2$, separated by the spin-flip frequency $\simeq 28.025$ GHz/T due to the magnetic moment of the positron, which, except for small bound-state corrections, is the same as for the free positron. Besides initial state preparation, which is discussed later, the method is identical to that already developed with great success for high precision measurements of the bound-electron g -factor in $^{12}\text{C}^{5+}$ [50], which have now reached a fractional uncertainty less than 3×10^{-11} [51, 52].

The apparatus consists of two adjacent Penning traps in a magnetic field of typically 5 tesla, a “precision trap” where the magnetic field is highly uniform, and where the measurement is carried out; and an “analysis trap”, where the magnetic field has an inhomogeneity with a quadratic spatial dependence $B \simeq B_0 + B_2 z^2$ [32]. In the analysis trap the positron spin state M_S is determined through the shift in axial frequency of the ion due to the interaction of its magnetic moment with the quadratic field gradient. This is known as the continuous Stern-Gerlach technique (CSG) [50, 53]. In contrast to the extreme difficulty of detecting a spin-flip of a bare antiproton, which has a 650 times smaller magnetic moment [10, 11, 54], the spin-flip of a bound positron produces an easily detectable change in axial frequency, enabling determination of M_S in 1 minute or less, in a magnetic field with modest inhomogeneity [52]. In the precision trap, the cyclotron frequency of the ion is measured by monitoring the evolution of the phase of the classical cyclotron motion [55, 56], while microwaves are applied at the expected spin-flip frequency, to make an attempt at inducing a positron spin-flip.

The measurement protocol consists of making an attempt at a spin-flip in the precision trap, while simultaneously measuring the cyclotron frequency, and then transferring the ion to the analysis trap to determine if a spin-flip had occurred in the precision trap. The process is repeated to map out spin-flip probability as a function of microwave drive frequency. Because the cyclotron frequency of the \bar{H}_2^- in the $(v, N) = (v, 0)$ state, $f_c = (1/2\pi)Bq(\bar{H}_2^-)/M(\bar{H}_2^-(v, 0))$, is measured simultaneously in the magnetic field B of the precision trap, the ratio of spin-flip frequency, f_s , to f_c is independent of B and is given by

$$\frac{f_s}{f_c} = \left| \frac{\bar{g}_e(\bar{H}_2^-(v, 0))}{2} \frac{q(e^+)}{m(e^+)} \frac{M(\bar{H}_2^-(v, 0))}{q(\bar{H}_2^-)} \right| \quad (1)$$

where $\bar{g}_e(\bar{H}_2^-(v, 0)) \simeq 2.002$, is the effective g -factor of the bound positron (defined so that the magnetic moment is $\bar{g}_e(\bar{H}_2^-(v, 0))\bar{\mu}_B M_S$, where $\bar{\mu}_B = \hbar q(e^+)/2m(e^+)$, with $q(e^+)/m(e^+)$ the charge-to-mass ratio of the free positron), and $q(\bar{H}_2^-)/M(\bar{H}_2^-(v, 0))$ is the charge-to-mass ratio of the \bar{H}_2^- ion, with allowance for the ro-vibrational energy. If one assumes the equality of $q(e^+)$ and $-q(e^-)$, of $-q(\bar{H}_2^-)$ and $q(H_2^+)$, and of $\bar{g}_e(\bar{H}_2^-(v, 0))$ and $-g_e(H_2^+(v, 0))$ [6], the \bar{H}_2^- to H_2^+ comparison is mainly sensitive to $m(e^+)/m(\bar{p}) - m(e^-)/m(p)$. Although higher precision can be obtained from vibrational spectroscopy on \bar{H}_2^- , see below, an uncertainty of 3×10^{-11} for a comparison of $m(e)/m(p)$ between matter and antimatter would already be competitive with the most precise comparisons of the masses of the proton and antiproton [8, 9] and of the electron and positron [5].

Ro-vibrational state and substate identification: Using a double-resonance technique the CSG technique can be applied more generally to determine the vibrational and rotational state of a simple paramagnetic molecular ion such as \bar{H}_2^- . In the case of even N , the Zeeman-hyperfine energies of \bar{H}_2^- in the high magnetic field of a Penning trap are given approximately by [40]

$$E(v, N; M_S, M_N; B) \simeq E(v, N) - \bar{g}_e(v, N)B\bar{\mu}_B M_S + \bar{g}_r(v, N)B\bar{\mu}_B M_N + \bar{\gamma}(v, N)M_S M_N, \quad (2)$$

where $\bar{g}_e(v, N)$ is the bound-positron g -factor, $\bar{g}_r(v, N)$ is the rotational g -factor, and $\bar{\gamma}(v, N)$ is the spin-rotation coupling constant, and B is the magnetic field. Hence, positron spin-flip transitions, which, in high B have the selection rule $\Delta M_S = \pm 1$, $\Delta M_N = 0$, have frequencies given by the energy difference

$$\Delta E(v, N, M_N; B) \simeq \bar{g}_e(v, N)B\bar{\mu}_B - \bar{\gamma}(v, N)M_N. \quad (3)$$

Now, while the dependence of $\bar{g}_e(v, N)$ on v and N is small, $\bar{\gamma}(v, N)$ has an easily resolvable dependence. For example, (for H_2^+) $\gamma(v, N)$ has the calculated values 42.162, 41.294, 39.572 and 38.748 MHz, for $(v, N) = (0, 2)$, $(0, 4)$, $(1, 2)$, and $(1, 4)$, respectively [57]. Hence, v , N , and M_N can be identified by determining the microwave frequency at which the positron spin-flip occurs, and comparing it with a theoretical value corresponding to the magnetic field, which can be determined from a measurement of cyclotron frequency. In most cases, sufficient resolution to identify the state could be achieved by inducing the spin-flips in the analysis trap, despite its inhomogeneous magnetic field. If $M_N = 0$, or if it is otherwise necessary to resolve ambiguities, additional information is obtained by inducing radio-frequency (RF) rotational hyperfine-Zeeman transitions with selection rules $\Delta M_N = \pm 1$, $\Delta M_S = 0$. These would be detected by looking for a change in frequency of a subsequent positron spin-flip. Examples of positron spin-flip transitions and a Zeeman-hyperfine transition are shown in Fig. 1.

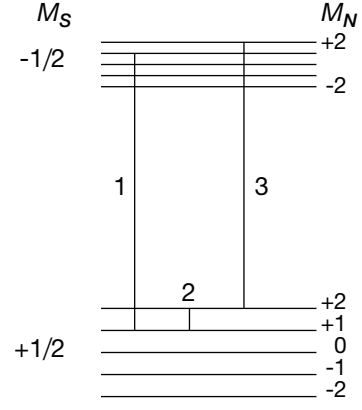


FIG. 1. Examples of positron spin-flip (Zeeman) transitions, 1, 3, and a rotational Zeeman-hyperfine transition, 2, in \bar{H}_2^- , for the case of $N = 2$ in a magnetic field of 5 T (not to scale). Using the Breit-Rabi formula [60] and Zeeman and Hyperfine coefficients from [57, 69], for $v = 0$, transitions 1, 2 and 3 have calculated frequencies of 140 082.6, 56.150, 140 040.4 MHz, respectively; and, for $v = 1$, 140 085.2, 54.499 and 140 045.6 MHz. This illustrates how M_N and v , (and also, by extension M_I and N) can be identified by measuring the positron spin-flip frequencies, with additional information given by measuring Zeeman-hyperfine transition frequencies. For H_2^+ the level structure is the same, but with the signs of M_S and M_N reversed.

The case for odd N with $I = 1$ is more complex, with three times as many substates. Nevertheless, the M_I state can be identified through the modification to the positron spin-flip frequency due to the nuclear spin hyperfine interaction, which adds several terms to the effective Hamiltonian, including a term $b(v, N)M_S M_I$, where $b(v, N)$ is the Fermi-contact hyperfine constant. Again, further identification results by inducing nuclear spin-flip transitions, with selection rules $\Delta M_I = \pm 1$, $\Delta M_S = 0$, $\Delta M_N = 0$. To minimize the time required for state identification, the microwaves or RF could be applied as pulses, at pre-calculated frequencies corresponding to the expected v, N , M_N , M_I states and the magnetic field.

A complementary method for detecting vibrational transitions, which is especially useful for $N = 0$ where the positron spin-flip frequency is insensitive to v , is to make use of the dependence of the cyclotron frequency on the vibrational mass-energy of the \bar{H}_2^- . This increases by 1.45, 2.81, and 4.09×10^{-10} for transitions between $v = 0$ and 1, 2, and 3, respectively. Although small, such shifts in cyclotron frequency are detectable, in a time scale of minutes to an hour, as shifts in a cyclotron frequency ratio [58, 59]. This can be implemented by comparison of the cyclotron frequencies of the \bar{H}_2^- and a D^- ion in the same precision trap, and then no analysis trap is needed. Alternatively, use can be made of the sensitivity of f_s/f_c to the \bar{H}_2^- mass as shown in Eqn. 1., and then another ion is not needed.

Hyperfine-Zeeman transitions and first-order field independent hyperfine transitions: Following from the above, see Fig.1, precision RF spectroscopy can be carried out on the rotational hyperfine-Zeeman $\Delta M_N = \pm 1$ transitions (for even and odd N), and nuclear-spin hyperfine-Zeeman transitions $\Delta M_I = \pm 1$ (for odd N), by making a try at inducing these transitions in the precision trap, and then moving the ion to the analysis trap and measuring the positron spin-flip frequency to detect if a change in M_N or M_I occurred. The magnetic field in the precision trap can be calibrated by measuring the cyclotron frequency simultaneously, or, by alternating with measurements of positron spin-flips. By taking suitable combinations of transitions, the interactions of the rotational and nuclear spin magnetic moments, with the external field (Zeeman), and with the positron spin magnetic moment (Hyperfine), can be separated [40]. Hence, comparisons of the magnetic moments of the antiproton and proton can be made, as has been done for the bare particles [10, 11, 54], but with the advantage of faster detection of the nuclear spin-flips; and also of the HFS, which additionally tests for equality of the antiproton and proton magnetization distributions. Further, for certain $\Delta M_I = \pm 1$ transitions, there are magnetic fields where the hyperfine-Zeeman transition frequencies are first-order independent of magnetic field. By adjusting the magnetic field to the appropriate values and using Ramsey type excitation schemes [60], this can be exploited to obtain measurements with fractional uncertainties less than 10^{-13} [61]. This fractional precision is competitive with the most precise measurements of hydrogen HFS using masers [62] and is more than three orders of magnitude higher than has currently been achieved using a cryogenic beam [23].

Ro-vibrational transitions: In the context of ro-vibrational spectroscopy of H_2^+ in an RF trap for fundamental constants and optical clocks, detailed analyses have been made of transition probabilities and systematic uncertainties for both 2E1 and E2 transitions, showing uncertainties can be controlled to the level of 10^{-16} or below [63–70]. While, for the highest precision, the possibility of trapping and sympathetically cooling an \bar{H}_2^- in an RF trap and performing quantum logic spectroscopy [71–73] should also be pursued, in the following it is shown that measurements in a Penning trap with uncertainties below 10^{-15} are already feasible.

As a specific example, consider the transition (0,2) to (1,2), with $\Delta M_S = 0$, $\Delta M_N = 0$, and $|M_S + M_N| = 5/2$, *i.e.*, between the stretched states, driven as an E2 transition at 65.4 THz by an ultra-stable laser. Assume that the \bar{H}_2^- ion is in a 5 T precision Penning trap, with axial (f_z), trap-modified cyclotron (f_{ct}) and magnetron frequencies (f_m) near 1 MHz, 35 MHz and 14 kHz, respectively; and that the axial and cyclotron motions are cooled using image currents to 20 mK, and the magnetron motion is cooled by magnetron-to-axial coupling [32, 74]

to 0.3 mK. For transverse laser irradiation, the ion's motion is then in the Lamb-Dicke regime with complete suppression of the first-order Doppler shift on the carrier [75]. The second-order Doppler shift leads to a Boltzmann distribution line shape with e^{-1} width of 60 mHz, consistent with a fractional uncertainty of 10^{-15} . Assuming a laser linewidth $\lesssim 0.1$ Hz, the transition can be induced using a 1 s pi-pulse with intensity of $\sim 6\mu\text{W mm}^{-2}$, with a fractional light shift of $\ll 10^{-17}$ [66]. The Stark shift, which is mainly due to the cyclotron motion and is proportional to the ion's temperature [76], is a factor of 10^{-3} smaller than the second-order Doppler shift. The Zeeman shift is $1.4 \times 10^5 \text{ Hz T}^{-1}$ [65, 69]. But, since a magnetic field stability of better than $10^{-9} \text{ hour}^{-1}$ and calibration to better than 10^{-9} can be routinely achieved in precision Penning traps, the resulting line broadening and uncertainty are < 1 mHz. Likewise, the quadrupole shift, which is also independent of the ion's temperature, and which can be estimated to be $\sim 1.0 \text{ Hz T}^{-2}$ [65], can be calibrated using knowledge of f_{ct} , f_z and f_m to better than 10^{-6} . Hence, besides laser frequency stability and metrology, the major limitation to precision is the second-order Doppler shift.

\bar{H}_2^- production and initial state selection: While it may be possible to synthesize \bar{H}_2^- in existing or developing antimatter apparatuses using the $\bar{p} + \bar{H} \rightarrow \bar{H}_2^- + \gamma$ [77, 78] or $\bar{H}(1s) + \bar{H}(n \geq 2) \rightarrow \bar{H}_2^- + e^+$ [79, 80] reactions, \bar{H}_2^- can be created more robustly through $\bar{H}^+ + \bar{p} \rightarrow \bar{H}_2^- + e^+$, by merging single cold \bar{H}^+ ions with a cold \bar{p} plasma. Although \bar{H}^+ ($\bar{p}e^+e^+$) has not yet been produced, this is a necessary goal of the ongoing GBAR antihydrogen gravity experiment [21], in which \bar{H}^+ will be made by double charge exchange between \bar{p} and positronium, using pulsed \bar{p} and positron beams [81]. The GBAR design goal is for one \bar{H}^+ to be created per AD cycle every 2 minutes [21]. Injected into a \bar{p} plasma with density of 10^6 cm^{-3} at $T \simeq 100 \text{ K}$, conditions already achieved [27, 28], an \bar{H}_2^- production rate of $1.4 \times 10^{-3} \text{ s}^{-1}$ can be estimated [82, 83]. However, because of the 180 times larger cross-section of the competing $\bar{H}^+ + \bar{p} \rightarrow \bar{H} + \bar{H}$, reaction [84, 85], an \bar{H}_2^- will be produced on average once per 180 \bar{H}^+ injections, with mixing times of $\sim 10 \text{ s}$.

$\bar{H}^+ + \bar{p} \rightarrow \bar{H}_2^- + e^+$ is exothermic by 1.896 eV. Hence, in a cool antiproton plasma the \bar{H}_2^- will be produced with $v \leq 8$ and $N \leq 27$. By transferring to a higher field (10T) Penning trap, and placing the ion in a large radius ($\gtrsim 4 \text{ mm}$) cyclotron orbit, the vibrational motion can be Stark quenched to $v = 0$ through the induced electric dipole moment [67], in a time scale ~ 1 week. Identification of v , N , M_N , and M_I proceeds by transferring to the analysis trap and determining the frequency of the positron spin-flip transition, with manipulation of M_N and M_I by hyperfine-Zeeman transitions. Reduction of N (and also v , if necessary) can then be effected using successive ro-vibrational transitions (v, N) to ($v', N - 2$),

again with state monitoring via the CSG technique in the analysis trap. The processes of making, state initialization, and measuring on a single \bar{H}_2^- may take many weeks. However, such time scales are already common for experiments on single ions in precision Penning traps [11, 54, 58].

Conclusion: Precision measurements on \bar{H}_2^- can provide tests of the CPT theorem that are more sensitive than those achievable with antihydrogen or the bare particles, particularly with regards to the positron(electron)/antiproton(proton) mass ratio, and

the positron(electron) antiproton(proton) hyperfine interaction. Practical schemes have been outlined for their implementation based on single-ion Penning trap techniques, including the continuous Stern-Gerlach effect and measurement of cyclotron frequency for state identification. The $\bar{H}^+ + \bar{p} \rightarrow \bar{H}_2^- + e^+$ reaction has been identified as a practical path for \bar{H}_2^- production.

The author thanks G. Gabrielse for enabling visits to CERN, and thanks members of the ATRAP collaboration for their hospitality. Support by the NSF under PHY-1403725 and PHY-1310079 is acknowledged.

-
- [1] G. Lüders, *Ann. Phys.* **2**, 1, (1957).
 - [2] R. Bluhm, V. A. Kostelecky, and N. Russell, *Phys. Rev. Lett.* **82**, 2254 (1999).
 - [3] Y. Yamazaki and S. Ulmer, *Ann. Phys. (Berlin)* **525**, 493 (2013).
 - [4] M. S. Safranova *et al.*, arXiv:1710.01833v1, submitted to *Reviews of Modern Physics*, 2017.
 - [5] M. S. Fee *et al.*, *Phys. Rev. Lett.* **70**, 1397 (1993).
 - [6] R. S. Van Dyck, Jr., P. B. Schwinberg, and H. G. Dehmelt, *Phys. Rev. Lett.* **59**, 26 (1987).
 - [7] D. Hanneke *et al.*, *Phys. Rev. Lett.* **100**, 120801 (2008).
 - [8] G. Gabrielse *et al.*, *Phys. Rev. Lett.* **82**, 3198 (1999).
 - [9] S. Ulmer *et al.*, *Nature* **524**, 196 (2015).
 - [10] J. DiSciaccia *et al.*, *Phys. Rev. Lett.* **110**, 130801 (2013).
 - [11] C. Smorra *et al.*, *Nature* **550**, 371 (2017).
 - [12] M. Hori *et al.*, *Science* **354**, 610 (2016).
 - [13] G. Gabrielse, in *Fundamental Symmetries*, ed. P. Bloch, P. Pavlopoulos, and R. Klapisch, (New York: Plenum) p59 (1987).
 - [14] M. H. Holzschteiter, M. Charlton, and M. M. Nieto, *Physics Reports* **402**, (2004).
 - [15] W. A. Bertsche *et al.*, *J. Phys. B: At. Mol. Opt. Phys.* **48**, 232001 (2015).
 - [16] D. W. Fitzakerley *et al.*, *J. Phys. B: At. Mol. Opt. Phys.* **49**, 064001 (2016).
 - [17] M. Ahmadi *et al.*, *Nature* **557**, 71 (2018).
 - [18] M. Ahmadi *et al.*, *Nature* **548**, 66 (2017).
 - [19] N. Kuroda *et al.*, *Nature Comm.* **5**, 3089 (2014).
 - [20] A. Kellerbauer *et al.*, *Nucl. Instr. Meth. B* **266**, 351 (2008).
 - [21] P. Perez *et al.*, *Hyperfine Interactions* **233**, 21 (2015).
 - [22] C. G. Parthey *et al.*, *Phys. Rev. Lett.* **107**, 203001 (2011).
 - [23] M. Diermaier *et al.*, *Nat. Commun.* **8**, 15749 doi:10.1038/ncomms15749 (2017).
 - [24] S. Maury, *Hyperfine Int.* **109**, 43, (1997).
 - [25] G. Gabrielse, S. L. Rolston, L. Haarsma, and W. Kells, *Phys. Lett. A* **129**, 38 (1988).
 - [26] G. Gabrielse *et al.*, *Phys. Rev. Lett.* **100**, 113001 (2008).
 - [27] G. B. Andresen *et al.*, *Nature* **468**, 673 (2010).
 - [28] P. Richerme *et al.*, *Phys. Rev. A* **87**, 023422 (2013).
 - [29] J. Walz *et al.*, *J. Phys. B: At. Mol. Opt. Phys.* **36**, 649 (2003).
 - [30] P. H. Donnan, M. C. Fujiwara, and R. Robicheaux, *J. Phys. B: At. Mol. Opt. Phys.* **46**, 025302 (2013).
 - [31] G. Gabrielse *et al.*, *Phys. Rev. Lett.* **57**, 2504 (1986).
 - [32] L. S. Brown and G. Gabrielse, *Rev. Mod. Phys.* **58**, 233 (1986).
 - [33] S. Rainville, J. K. Thompson, and D. E. Pritchard, *Science* **303**, 334 (2004).
 - [34] E. G. Myers, A. Wagner, H. Kracke, and B. A. Wesson, *Phys. Rev. Lett.* **114**, 013003 (2015).
 - [35] G. Gabrielse, *Advances in Atomic, Molecular, and Optical Physics* **45**, 1 (2001).
 - [36] S. Sellner *et al.*, *N. J. Phys.* **19**, 083023 (2017).
 - [37] E. G. Myers, *Int. J. Mass Spectrometry*, **349-350**, 107 (2013).
 - [38] A. Carrington, I. R. McNab, and C. A. Montgomerie, *J. Phys. B: At. Mol. Opt. Phys.* **22**, 3551 (1989).
 - [39] R. Moss, *Mol. Phys.* **80**, 1541 (1993).
 - [40] J. M. Brown and A. Carrington, *Rotational Spectroscopy of Diatomic Molecules*, Cambridge, 2003. 316 (2003).
 - [41] A. Posen, A. Dalgarno, and J. Peek, *At. Data Nucl. Data Tables* **28**, 265 (1983).
 - [42] H. O. Pilon and D. Baye, *Phys. Rev. A* **88**, 032502 (2013).
 - [43] A. D. Ludlow, M. M. Boyd, J. Ye, E. Peik, and P. O. Schmidt, *Rev. Mod. Phys.* **87**, 637 (2015).
 - [44] N. Huntemann, C. Sanner, B. Lipphardt, Chr. Tamm, and E. Peik, *Phys. Rev. Lett.* **116**, 063001 (2016).
 - [45] S. Peil and G. Gabrielse, *Phys. Rev. Lett.* **83**, 1287 (1999).
 - [46] D. J. Heizen and D. J. Wineland, *Phys. Rev. A* **42**, 2977 (1990).
 - [47] M. Bohman *et al.*, *J. Mod. Optics*, DOI: 10.1080/09500340.2017.1404656 (2017).
 - [48] A. Kellerbauer and J. Walz, *N. J. Phys.* **8**, 45 (2006).
 - [49] P. Yzombard, M. Hamamda, S. Gerber, M. Doser, and D. Comparat, *Phys. Rev. Lett.* **114**, 213001 (2015).
 - [50] G. Werth, H. Häffner, and W. Quint, *Adv. Atomic, Molec. Optical Physics* **48**, 191 (2002).
 - [51] S. Sturm *et al.*, *Nature (London)* **506**, 467 (2014).
 - [52] F. Köhler, S. Sturm, A. Kracke, W. Quint, and K. Blaum, *J. Phys. B: At. Mol. Opt. Phys.* **48**, 144032 (2015).
 - [53] H. Dehmelt, *Proc. Natl. Acad. Sci. USA* **83**, 2291 (1986).
 - [54] G. Schneider *et al.*, *Science* **358** (6366), 1081 (2017).
 - [55] E. A. Cornell *et al.*, *Phys. Rev. Lett.* **63**, 1674 (1989).
 - [56] S. Sturm, A. Wagner, B. Schabinger, and K. Blaum, *Phys. Rev. Lett.* **107**, 143003 (2011).
 - [57] V. I. Korobov, L. Hilico, and J.-Ph. Karr, *Phys. Rev. A* **74**, 040502(R), (2006).
 - [58] S. Hamzeloui, J. A. Smith, D. J. Fink, and E. G. Myers, *Phys. Rev. A* **96**, 060501(R) (2017).
 - [59] J. A. Smith, S. Hamzeloui, D. J. Fink, and E. G. Myers,

- Phys. Rev. Lett. **120**, 143002 (2018).
- [60] N. F. Ramsey, *Molecular beams*, Clarendon Press, Oxford, 1956.
 - [61] J. J. Bollinger, J. D. Prestage, W. M. Itano, and D. J. Wineland, Phys. Rev. Lett. **54**, 1000 (1985).
 - [62] P. Petit, M. Desaintfuscien, and C. Audoin, Metrologia **16**, 7 (1980).
 - [63] L. Hilico, N. Billy, B. Grémaud, and D. Delande, J. Phys. B: At. Mol. Opt. Phys. **34**, 491 (2001).
 - [64] J.-Ph. Karr, L. Hilico, J. C. J. Koelemeij, and V. I. Korobov, Phys. Rev. A **94**, 050501(R) (2016).
 - [65] S. Schiller, D. Bakalov, and V. I. Korobov, Phys. Rev. Lett. **113**, 023004 (2014).
 - [66] J.-Ph. Karr, J. Mol. Spec. **300**, 37 (2014).
 - [67] S. Schiller, D. Bakalov, A. K. Bekbaev, and V. I. Korobov, Phys. Rev. A **89**, 052521 (2014).
 - [68] J.-P. Karr *et al.*, Phys. Rev. A **77**, 063410 (2008).
 - [69] J.-P. Karr, V. I. Korobov, and L. Hilico, Phys. Rev. A **77**, 062507 (2008).
 - [70] D. Bakalov and S. Schiller, Appl. Phys. B **114**, 213 (2014).
 - [71] C. W. Chou, D. B. Hume, J. C. J. Koelemeij, D. J. Wineland, and T. Rosenband, Phys. Rev. Lett. **104**, 070802 (2010).
 - [72] C. W. Chou, C. Kurz, D. B. Hume, P. N. Plessow, D. R. Leibbrandt, and D. Leibfried, Nature **545**, 203 (2017).
 - [73] D. Leibfried, Appl. Phys. B **123**:10 (2017).
 - [74] E. A. Cornell, R. M. Weisskoff, K. R. Boyce, and D. E. Pritchard, Phys. Rev. A **41**, 312 (1990).
 - [75] D. J. Wineland *et al.*, J. Res. Natl. Inst. Stand. Technol. **103**, 259 (1998).
 - [76] H. S. Margolis, J. Phys. B: At. Mol. Opt. Phys. **42**, 154017 (2009).
 - [77] D. R. Bates, Mon. Not. Roy. Astr. Soc. **111**, 303 (1951).
 - [78] M. C. Zammit *et al.*, Astr. Phys. J. **851**, 64 (2017).
 - [79] R. K. Janev, D. Reiter and U. Samm, *Collision processes in low-temperature hydrogen plasmas*, Berichte des Forschungszentrums Jülich **4105**, ISSN: 0944-2952.
 - [80] J. M. C. Rawlings, J. E. Drew, and M. J. Barlow, AIP Conf. Proc. **312**, 437 (1994).
 - [81] J. Walz and T. Hänsch, General Relativity and Gravitation **36**, 561 (2004).
 - [82] X. Urbain, A. Giusti-Suzor, D. Fussen, and C. Kubach, J. Phys. B: At. Mol. Phys. **19**, L273 (1986).
 - [83] G. Poulaert, F. Brouillard, W. Claeys, J. W. McGowan, and G. Van Wassenhove, J. Phys. B: At. Mol. Phys. **11**, L671 (1978).
 - [84] M. Stenrup, Å. Larson, and N. Elander, Phys. Rev. A **79**, 012713 (2009).
 - [85] S. M. Nkambule, N. Elander, Å. Larson, J. Lecointre, and X. Urbain, Phys. Rev. A **93**, 032701 (2016).